HHS Public Access

Author manuscript

J Immunol. Author manuscript; available in PMC 2016 December 01.

Published in final edited form as:

J Immunol. 2015 December 1; 195(11): 5237–5250. doi:10.4049/jimmunol.1500959.

Expression of Cationic Amino Acid Transporter 2 (CAT2) Is Required for Myeloid Derived Suppressor Cell-Mediated Control of T Cell Immunity

Cansu Cimen Bozkus[*], **Bennett D. Elzey**[*], **Scott A. Crist**[*], **Lesley G. Ellies**[†], and **Timothy L. Ratliff**[*]

[*]Comparative Pathobiology Department and Purdue University Center for Cancer Research, Purdue University, West Lafayette, IN 47907

[†]Department of Pathology, University of California, San Diego, La Jolla, CA 92093

Abstract

Myeloid derived suppressor cells (MDSC) are a heterogeneous population of immature cells that expand during benign and cancer-associated inflammation and are characterized by their ability to inhibit T cell immunity. Increased metabolism of L-Arginine, through the enzymes arginase 1 (ARG1) and nitric oxide synthase 2 (NOS2), is well documented as a major MDSC suppressive mechanism. Therefore, we hypothesized that restricting MDSC uptake of L-Arginine is a critical control point to modulate their suppressor activity. Using murine models of prostate specific inflammation and cancer, we have identified the mechanisms by which extracellular L-Arginine is transported into MDSC. We have shown that MDSC recruited to localized inflammation and tumor sites upregulate cationic amino acid transporter 2 (*Cat2*), coordinately with *Arg1* and *Nos2*. *Cat2* expression is not induced in MDSC in peripheral organs. CAT2 contributes to the transport of L-Arginine in MDSC and is an important regulator of MDSC suppressive function. MDSC that lack CAT2 have significantly reduced suppressive ability *ex vivo* and display impaired capacity for regulating T cell responses *in vivo* as evidenced by increased T cell expansion and decreased tumor growth in $Cat2^{-/-}$ mice. The abrogation of suppressive function is due to low intracellular L-Arginine levels, which leads to the impaired ability of NOS2 to catalyze L-Arginine dependent metabolic processes. Together, these findings demonstrate that CAT2 modulates MDSC function. In the absence of CAT2, MDSC display diminished capacity for controlling T cell immunity in prostate inflammation and cancer models, where the loss of CAT2 results in enhanced antitumor activity.

Introduction

Hematopoiesis is altered in inflammation and cancer. Such pathological conditions stimulate myelopoiesis, inhibit differentiation of immature myeloid cells and induce their activation (1, 2). This heterogeneous population of immature myeloid cells, called myeloid derived

Address correspondence and reprint requests to Dr. Timothy L. Ratliff, Comparative Pathobiology Department, Purdue University, 201 S., University St. Hansen Life Sciences Research Building, West Lafayette, IN 47907-2064. tlratliff@purdue.edu, Phone number: 765-494-9129, Fax number: 765-494-9193.

suppressor cells (MDSC), is important for controlling inflammation and notably, have been shown to be recruited to benign and cancer associated inflammation sites to block T cell immunity (1). MDSC-mediated suppression facilitates tumor progression and is associated with worse prognosis, increased metastatic tumor burden and decreased survival of cancer patients (3, 4). Consequently, blockade of MDSC suppressor capacity has been suggested to be an essential component for improving antitumor immune responses (5). Therefore, MDSC are a critical target for cancer immunotherapy. Additionally, MDSC have been shown to play beneficial roles in autoimmune diseases (6-8). Unfortunately, current strategies for controlling MDSC suppressor function have not found clinical application.

In mice, MDSC are characterized by coexpression of CD11b and Gr-1 surface markers. MDSC comprise heterogeneous mixtures of myeloid cells at early differentiation stages. The most recognized MDSC subpopulations are monocytic (M-MDSC) and granulocytic (G-MDSC) subsets, identified as $CD11b^{+}Ly6C^{high}Ly6G^{-}$ and $CD11b^{+}Ly6C^{low}Ly6G^{+}$, respectively (1). It is generally accepted that M-MDSC are the dominant suppressor phenotype but depending on the tumor model, G-MDSC may mediate significant suppression as well (9, 10). MDSC use multiple mechanisms to mediate T cell suppression. Increased expression and activities of arginase 1 (ARG1) and inducible nitric oxide synthase 2 (NOS2) are well established as the hallmarks for MDSC suppressive function (11). Both enzymes use L-Arginine (L-Arg) as a common substrate and deplete L-Arg from the microenvironment, produce nitric oxide (NO), reactive oxygen species (ROS) and reactive nitrogen species (RNS), which mediate T-cell suppression (11). Excessive ARG1 and NOS2 activities in MDSC require L-Arg import (12). Despite its importance as the unique substrate for ARG1 and NOS2, the mechanism by which L-Arg is transported into MDSC and the impact of L-Arg transport on suppressor function has not been defined.

There are four transporter systems for L-Arg uptake through mammalian cellular membranes: y^{+}, $y^{+}L$, $b^{o,+}$, $B^{o,+}$ (13). Among these systems, y^{+} shows higher selectivity for cationic amino acids, such as L-Arg, and is considered as the major route for L-Arg entry into cells (14). y^{+} system comprises four carrier proteins: CAT1 – CAT4. The specific functions of CAT3 and CAT4 are not well characterized. CAT1 is ubiquitously expressed, with the exception of adult liver. However, CAT1 transport of L-Arg is slow and therefore cells with a high demand of L-Arg induce CAT2 expression to provide rapid transport of L-Arg to meet functional requirements (15). For example, activated macrophages upregulate CAT2 expression upon activation and the lack of CAT2 results in a significant decrease in L-Arg transport and NO production, indicating CAT2 is required for sustained NOS2 activity (16, 17). Mature tumor-associated myeloid cells, $CD11b^{+}Gr\text{-}1^{-}$, also display increased CAT2 expression and the concomitant L-Arg uptake (18). Although CAT2 is well studied in the context of L-Arg transport in various cell types, its importance in transportation of L-Arg in MDSC and its role as a regulator of MDSC suppressive function is unknown. Using murine models of prostate specific inflammation and cancer, we investigated the role of CAT2 in MDSC suppressive activity. We provide evidence that *Cat2* is coordinately induced with *Arg1* and *Nos2*. The data show that CAT2 is an active transporter of L-Arg in MDSC and its function is required for optimal suppressive activity.

CAT2 deficient-MDSC display an impaired capacity for regulating T cell responses both *ex vivo* and *in vivo*.

Materials and Methods

Mice

C57BL/6 mice were purchased from Jackson Laboratories. *Cat2*$^{-/-}$ and POET-3 mice were generated as described previously (16, 19). *Cat2*$^{-/-}$POET-3 mice were generated by breeding *Cat2*$^{-/-}$ and POET-3 mice. Rag$^{-/-}$Thy1.1^{+} ovalbumin specific T cell (OTI) mice were generated by breeding Thy1.1^{+}OTI mice and Rag$^{-/-}$ mice purchased from Jackson Laboratories. Both female and male mice between 7 and 12 weeks of age were used for all tumor studies. For POET-3 experiments only male mice were used. All animal experiments for this study were approved by the Purdue University Animal Care and Use Committee.

Animal models

C57BL/6 and *Cat2*$^{-/-}$ mice were used for tumor studies. For prostate cancer studies, 1× 10^6 RM1 prostate cancer cells were injected intraperitoneally. Mice were sacrificed 6-7 days after tumor cell inoculation. For the bladder cancer model, 5× 10^5 MB49 bladder cancer cells were injected subcutaneously in the flank area. Mice were sacrificed after 14 days when tumors reached 1.5 cm in diameter. For tumor growth experiments, mice were injected with 3× 10^6 Fico/Lite (Atlanta Biologicals) purified EG7 or EL4 cells subcutaneously in the flank area or intradermally in the shoulder area. After 7 days 1-1.5× 10^6 activated OTI cells were injected intravenously. For the Winn assay, 3× 10^6 EG7 or EL4 cells were injected intradermally in the shoulder area with or without 10^4 activated OTI cells in the presence or absence of 10^4 CAT2$^{+/+}$ or CAT2$^{-/-}$ CD11b^{+}Gr-1^{+} cells isolated from the ascites of RM1 mice. Tumor size was measured using calipers and calculated by the formula [(small diameter)^2 × (large diameter) × 0.5]. POET-3 and *Cat2*$^{-/-}$ POET-3 mice were used for inflammation studies. Prostate inflammation was induced by intravenous injection of 5× 10^6 *in vitro* activated (48 h) OTI cells into POET-3 mice. Mice were sacrificed 5 days after the induction of inflammation. For the adoptive transfer studies, 2 days after the induction of inflammation POET-3 mice received (i.p.) 4× 10^6 MDSC generated by culturing bone marrow cells with GM-CSF (40 ng/ml) and IL-6 (40 ng/ml) (purchased from Peprotech) for 5 days.

Cell isolation and generation

Bone marrow was collected from femurs and tibias. Spleens were harvested and ground using frosted slides. Cells from ascitic tumors were collected by flushing the peritoneal cavity with 10 ml PBS. Cells from solid tumors were collected by digesting the minced tissue at 37°C for 1 hour in media containing Collagenase D (2 mg/ml, Roche Diagnostics) and DNAse I (10 μg/ml, Sigma-Aldrich). Cells from prostate glands were obtained by harvesting and pooling anterior, ventral and dorsolateral lobes of prostates and minced tissues were digested for an hour at 37°C in media containing Collagenase D (2 mg/ml). Red blood cells were lysed by using ACK buffer and cells were passed through a 70 μm filter. OTI cells were isolated from the spleens of Rag$^{-/-}$OTI mice and activated by culturing in RPMI 1640 media containing SIINFEKL (1 μg/ml, Ova peptide 257-264, American peptide)

and 2-ME (55 μM). Activated OTI were purified by Fico/Lite. Macrophages were obtained by collecting cells from mice by washing the peritoneal cavity with 10 ml PBS 5 days after thioglycollate injection (i.p.). Cells were cultured and unattached cells were removed after 2 hours. Macrophages were then cultured for another 17 hours in the absence or presence of LPS (100 ng/ml, Sigma-Aldrich) and IFN-γ (25 ng/ml, Peprotech). For *in vitro* activation of MDSC, $CD11b^{+}Gr\text{-}1^{+}$ cells were isolated from bone marrow by FACS and were cultured for 3 days with GM-CSF (40 ng/ml), IFN-γ (25 ng/ml) and IL-13 (33 ng/ml, Peprotech).

Flow cytometry

Single cell suspensions were incubated with TruStain fcX (Clone:93) and stained with conjugated antibodies. MDSC were labelled with anti-CD11b (Clone: M1/70), anti-Gr-1 (Clone: RB6-8C5), anti-Ly-6C (Clone: HK1.4) and anti-Ly-6G (Clone: 1A8). T cells were labelled with anti-CD45 (Clone: 30-F11), anti-CD8a (Clone: 53-6.7) and anti-CD90.1 (Clone: OX-7). To measure IFN-γ production by OTI, cells were cultured for 6-8 hours in the presence of SIINFEKL and Golgi Stop (BD Biosciences). After staining for surface antigens, cells were prepared for intracellular staining using the CytoFix/CytoPerm™ kit (BD Biosciences) and stained with anti-IFN-γ (Clone: XMG1.2). Antibodies were purchased from BioLegend and used at 2 μg/ml concentration. OTI proliferation was measured using BrdU Flow Kit (BD Biosciences) or Click-iT® EdU Flow Cytometry Assay Kit (Molecular Probes, Life Technologies) according to the manufacturer's instructions. For ARG1 and NOS2 protein detection, following surface antigen staining cells were fixed and permeabilized using BD CytoFix/CytoPerm™ kit. Cells were then stained for ARG1 and NOS2 for 30 minutes at room temperature. ARG1 staining was performed in 20 μl of 25 μg/ml PE-conjugated anti-ARG1 polyclonal antibody or the isotype control PE-conjugated polyclonal sheep IgG (R&D Systems). For NOS2 detection, APC conjugated anti-NOS2 monoclonal antibody (eBioscience, Clone: CXNFT) and the APC conjugated mouse-IgG2a isotype control (Clone: RMG2a-62) were used at 10 μg/ml. All analyses were performed using BD FACSCanto II and data were analyzed using FlowJo software (Tree Star). All cell sorting was performed using a BD FACSAria III. Sort purities were above 95%.

Quantitative real time PCR

Total RNA was isolated from cells using the E.Z.N.A. Total RNA Kit I (Omega Bio-tek)and cDNA synthesis was performed using qScriptTM cDNA SuperMix (Quanta Biosciences) according to the manufacturer's instructions. Multiplex qRT-PCR was performed using PerfeCTa® FastMix® II (Quanta Biosciences), PrimeTime® qPCR gene probes (IDT) including Arg1 (Mm.PT.58.8651372), Nos2 (Mm.PT.58.43705194), Slc7a2 (Mm.PT. 58.28825099) and endogenous control 18s rRNA (Applied Biosystems). Relative mRNA expression was calculated by the formula $2^{-[Ct(gene) - Ct(18s\ rRNA)]}$, where Ct is the threshold cycle value.

L-Arginine transport assays

Isolated MDSC were cultured overnight with GM-CSF (40 ng/ml), IFN-γ (25 ng/ml), IL-13 (33 ng/ml). Peritoneal macrophages were cultured with LPS (100 ng/ml) and IFN-γ (25 ng/ml) for 17 hours. Transport assays were carried out at 25°C in a buffer containing 118.5

mM NaCl, 5.6 mM KCl, 1.3 mM $CaCl_2$, 0.6 mM $MgCl_2$, 11.1 mM glucose, 0.03 mM EDTA, 0.06 mM L-Ascorbic Acid and 20 mM HEPES. Transport through the y^+ system was blocked by pretreating cells with *N*-ethyl maleimide (NEM) (5 mM) (Sigma-Aldrich) at 25°C for 5 min. To block transportation through the y^+L system 5 mM L-Leucine (L-Leu) was added to the transport buffer. Cells were pulsed with L-^{3}[H]-Arginine (6μCi/ml, PerkinElmer) for 3 min and were washed with stop solution (transport buffer containing 10 mM nonradioactive L-Arg). Cells were then lysed with 4% Triton X-100 and the uptake was measured using a scintillation counter. The protein concentration of cell lysates was measured using the Bradford assay (Sigma-Aldrich) according to the manufacturer's instructions. Uptake was represented as CPM/mg protein for normalization purposes.

MDSC functional assays

Sorted MDSC or MDSC subsets were co-cultured in 96-well U bottom plates with OTIs (10^5 cells/well) preactivated for 8 hours (or naïve, where indicated) in media containing the cognate antigen SIINFEKL. OTI proliferation was measured by determining BrdU or EdU incorporation after 18 hours for short-term assays and 48-72 hours for long-term assays. BrdU and EdU were added 6 and 2 hours before harvest, respectively. BrdU and EdU incorporation were measured by flow cytometry. Where indicated LNMMA (0.5 mM, Calbiochem), nor-NOHA (0.5 mM, Calbiochem) and NAC (1 or 10 mM, Sigma-Aldrich) were added to the suppression assay at the beginning of co-culture. The percent suppression was calculated as [[1-(proliferation with MDSC)/(proliferation without MDSC)]× 100]. IFN-γ production was measured by intracellular IFN-γ staining for flow cytometry.

Measurement of nitrite, ROS and urea

Sorted cells were cultured for 24 hours with or without LPS (100 ng/ml) and IFN-γ (25 ng/ml). Nitrite formation was quantified using the Standard Griess Assay (Molecular Probes, Life Technologies) according to the manufacturer's instructions. Reactive oxygen species (ROS) formation was measured using DCFDA – Cellular reactive oxygen species detection assay kit (abcam) according to the manufacturer's instructions. In the arginase assay, sorted cells were lysed in 0.1 % Triton X-100 containing protease inhibitors (Roche) at 10^7 cells/ml and incubated at room temperature for 30 minutes. Subsequently, equal volume of 10 mM $MnCl_2$ and 25 mM Tris-HCl (pH 7.5) were added. Following 10 min incubation at 55 °C, equal volume of 0.5 M L-Arginine (pH 9.7) was added. 5 μl of lysates were incubated for 2 hours at 37°C. BioAssay Systems Quantichrome Urea Assay Kit, which detects urea and citrulline equivalently (20), wasused according to the manufacturer's instructions in order to determine arginase activity.

Statistical analysis

Data were presented as mean ± SEM. Statistical analyses were performed using GraphPad Prism software. p values were calculated using *Student's t test* and one-way ANOVA with Bonferroni's post-test when two or multiple groups were compared, respectively. Differences were considered significant where $p < 0.05$.

Results

Cat2 expression is induced in MDSC upon acquisition of suppressive function

To assess if *Cat2* expression is upregulated in MDSC upon gaining suppressive activity, we utilized an *in vitro* system in which we isolated $CD11b^{+}Gr\text{-}1^{+}$ cells from bone marrow and cultured them with activating cytokines (IFN-γ, IL-13 and GM-CSF) for 3 days (21). After 3 days of culture with cytokines MDSC upregulated *Arg1* and *Nos2* expression and could suppress T cells (Fig. 1A,B and 3A). We compared *Cat2* expression levels in $CD11b^{+}Gr\text{-}1^{+}$ cells that were cultured with or without activating cytokines. We saw that *Cat2* expression was induced in activated MDSC in parallel with *Arg1* and *Nos2* expression (Fig. 1C). In order to evaluate if the induction of *Cat2* expression is coordinately regulated with *ArgI* and *Nos2* induction, we measured gene expression of *in vitro* activated MDSC after 24, 48 and 72 hours of culture. The data show that the kinetics of *Cat2* induction in MDSC parallels the induction of *ArgI* and *Nos2* expression (Fig. 1D). Next, we evaluated *Cat2* expression levels in $CD11b^{+}Gr\text{-}1^{+}$ cells isolated from tumor bearing mice. We previously published that only MDSC at the tumor site, but not at peripheral sites such as spleen, have immediate suppressive capacity (22). In order to investigate if *Cat2* is indeed induced only in MDSC with suppressive function, we compared *Cat2* expression in $CD11b^{+}Gr\text{-}1^{+}$ cells isolated from the spleen and tumor sites of tumor bearing mice. To this end, we utilized a tumor model in which RM1 murine prostate cancer cells were injected intraperitoneally (i.p.) into $Cat2^{+/+}$ mice (23). Six days after tumor inoculation, $CD11b^{+}Gr\text{-}1^{+}$ population was significantly expanded in the spleen and ascites of RM1 bearing mice compared to the naïve control mice (Fig. 2A). $CD11b^{+}Gr\text{-}1^{+}$ cells were isolated from the spleen and as cites of RM1 i.p. tumor bearing mice and from the spleen of naïve mice. Only the MDSC isolated from the tumor site, with immediate suppressive function, but not from spleens of naïve or tumor bearing mice had elevated *Cat2* expression (Fig. 2B). In addition we examined *Cat2* expression in MDSC subsets (Fig. 2C). Both monocytic ($CD11b^{+}Ly6C^{high}Ly6G^{-}$) (M-MDSC) and granulocytic ($CD11b^{+}Ly6C^{low}Ly6G^{+}$) (G-MDSC) subsets at the tumor site displayed high *Cat2* expression unlike splenic counterparts (Fig. 2D). These data show that *Cat2* expression is induced in MDSC with immediate suppressive function.

CAT2 regulates MDSC suppressive function

To evaluate if CAT2 regulates MDSC suppressive function, we compared the suppressive ability of $Cat2^{+/+}$, $Cat2^{+/-}$ and $Cat2^{-/-}$ MDSC *in vitro*. After 3 days of culture with activating cytokines, bone marrow $CD11b^{+}Gr\text{-}1^{+}$ cells were co-cultured with naïve OTI cells, ovalbumin (OVA) specific $CD8^{+}$ T cells, in the presence of activating peptide. $Cat2^{-/-}$, but not $Cat2^{+/-}$ MDSC, displayed significantly reduced suppressive function compared to $Cat2^{+/+}$ MDSC at all ratios (Fig. 3A). Since CAT2 needs to be completely absent in order to reduce suppressive capacity, for the rest of the study we utilized $Cat2^{+/+}$ (WT) and $Cat2^{-/-}$ (KO) MDSC. Next, we investigated if $Cat2^{-/-}$ MDSC isolated from tumor sites had lower suppressive function. We isolated $CD11b^{+}Gr\text{-}1^{+}$ cells from spleen and as cites of i.p. RM1 bearing WT and KO mice. Accumulation of $CD11b^{+}Gr\text{-}1^{+}$ cells at the tumor site, spleen and bone marrow was comparable in both WT and KO animals (not shown). To measure suppressive activity, we cultured isolated $CD11b^{+}Gr\text{-}1^{+}$ cells with pre-activated OTI cells for 18 hours at differing ratios. This is a short-term assay and in this assay only MDSC with

immediate suppressor function are able suppress OTI proliferation (22). As expected, precursor cells from spleen did not suppress OTI proliferation in 18 hours, but WT MDSC from tumor site were suppressive. Similar to *in vitro* activated MDSC, MDSC isolated from tumor site possessed significantly reduced ability to suppress OTI proliferation in the absence of CAT2, where suppression by $CAT2^{-/-}$ MDSC was observed only at a 2:1 MDSC:OTI ratio (Fig. 3B). Evaluation of the suppressive capacity of MDSC in a long-term (48 hours) suppression assay also demonstrated a similar reduced suppressive capacity of KO MDSC (Fig. 3C). In addition we determined intracellular IFN-γ levels of OTI cells at the end of the culture. We observed that co-culture with WT MDSC resulted in fewer OTI cells that displayed intracellular IFN-γ, further confirming the decreased suppressive capacity of CAT2-ablated MDSC (Fig. 3D). To verify that our observations were not limited to the RM1 ascites model, we implanted mice with MB49 bladder cancer cells subcutaneously and monitored CAT2 dependent MDSC suppressive function in a 48-hour culture (Supp. Figure 1A). MDSC isolated from both tumor site and spleens of MB49 tumor bearing animals had lower suppressive activity in the absence of CAT2, suggesting that our observations are broadly applicable. We also evaluated the suppressive capacity of MDSC subsets individually. Both M-MDSC and G-MDSC subsets displayed diminished suppressive capacity in the absence of CAT2 (Fig. 3E). In addition to tumor site MDSC, we utilized MDSC subsets isolated from spleen and bone marrow. In a long-term assay, prolonged culture time enables MDSC from peripheral sites to gain suppressive function due to exposure to endogenous and T cell-secreted activating factors. Therefore, unlike the results from short-term suppression assays, spleen and bone marrow MDSC are expected to suppress T cells in a long-term assay (22). Accordingly, we observed that MDSC from spleen and bone marrow displayed reduced suppressive action without CAT2 (Supp. Figure 1B). These results demonstrate that CAT2 is an important regulator of MDSC suppressive capacity. In the absence of CAT2 MDSC display significantly reduced levels of suppressive activity.

CAT2 mediates L-Arginine transportation in MDSC

Because *Cat2* expression is elevated in parallel to L-Arg-dependent activities of*Arg1* and *Nos2* (12), we asked whether CAT2 was modulating L-Arg intake in MDSC. To measure L-Arg intake we used MDSC isolated from ascites of i.p. RM1 bearing WT and KO mice. It has been reported that CAT2 plays a crucial role in L-Arg transport of activated thioglycollate-elicited peritoneal macrophages (16). Therefore, we used macrophages from WT and KO mice as a control. We measured L-^{3}[H]-Arginine uptake in activated macrophages (Fig. 4A) and tumor site MDSC (Fig. 4B). As reported (16), in activated macrophages when CAT2 was absent, the reduction in L-Arg uptake was about 90%. As we anticipated, in MDSC L-Arg uptake was significantly lower in the absence of CAT2. Interestingly in MDSC, L-Arg transport was much lower than macrophages when standardized to protein levels and CAT2-mediated L-Arg transport corresponded to only about 20% of total transport. Even so, CAT2-mediated transport is essential for optimal suppressive activity. There are multiple transportation systems that carry extracellular L-Arg into the cell. In order to eliminate the possibility that in KO MDSC an alternate transporter is over-expressed and is compensating for the lack of CAT2, we investigated the expression levels of all members of L-Arg transporter systems in WT and KO MDSC by qPCR (Supp.

Figure 2). Data show that none of the amino acid transporters that can transport L-Arg are over-expressed in KO MDSC. Additionally, data revealed that in MDSC, only the members of y^+ and y^+L systems are expressed. We could not detect any expression of transporters that are members of $b^{0,+}$ and $B^{0,+}$ systems. Next, we evaluated the specific contribution of y^+ and y^+L systems in L-Arg uptake in MDSC. To this end, we utilized an inhibitor, *N*-ethyl maleimide (NEM), that can block L-Arg transportation through the y^+ system. NEM treatment blocked about 25% of total transport in intact MDSC. Importantly, the inhibition of L-Arg transport in intact MDSC upon the blockade of y^+ system was comparable to the inhibition in $CAT2^{-/-}$ MDSC, indicating that CAT2 is the major y^+ system transporter in MDSC. Accordingly, the total L-Arg transportation through CAT1, CAT2 and CAT4 was significantly lower than L-Arg uptake through CAT2 (Fig. 4C). In order to determine the contribution of y^+L system, we measured L-Arg uptake in the presence or absence of 5 mM L-Leu. Addition of excessive amounts of L-Leu to the transportation medium competitively blocks L-Arg transportation through the y^+L system. Data showed that the y^+L system carries out about 25% of the L-Arg uptake in MDSC and in accordance with the gene expression data both WT and KO MDSC had similar y^+L system activities (Fig. 4D). Together, these results show thatCAT2 is an important carrier of L-Arg in MDSC, yet it is not the only transporter that mediates L-Arg uptake.

Lower suppressive capacity of $CAT2^{-/-}$MDSC is due to reduced NO production

Next, we evaluated the mechanisms through which CAT2 modulates MDSC suppressor function. One of the major suppressive mechanisms in MDSC is the production of NO by NOS2. Since NOS2 uses L-Arg as its substrate to produce NO and CAT2 ablated MDSC have lower L-Arg uptake, we hypothesized that CAT2 KO MDSC have reduced NO production. To test this, we measured nitrite production in WT and KO MDSC and MDSC subsets using a standard Griess reaction (Fig. 5A,B). We used activated macrophages as a control, since it is reported that in the absence of CAT2, activated macrophages have a 92% reduction in NO production (16) (Fig. 5C). As expected, WT MDSC produced significantly higher levels of NO. To eliminate the possibility that reduced NO formation in $CAT2^{-/-}$ MDSC could be due to diminished NOS2 expression in the absence of CAT2, we inspected NOS2 protein levels in $CAT2^{+/+}$ and $CAT2^{-/-}$ MDSC subsets. Data showed that NOS2 expression was similar in $CAT2^{+/+}$ and $CAT2^{-/-}$ MDSC. Notably, in agreement with gene expression data (Fig. 2D), NOS2 protein expression was also mostly confined to the M-MDSC subset (Fig. 5D). Freshly isolated MDSC from $CAT2^{+/+}$ and $CAT2^{-/-}$ also were tested for NOS2 levels and although lower levels were present, the levels were comparable between the two phenotypes (Supp. Figure 3). Together, these data indicate that NOS2 expression in MDSC is not modulated by CAT2 and hence the reduced NO formation in $CAT2^{-/-}$ MDSC is likely to be due to diminished L-Arg uptake.

Another important suppressive mechanism MDSC use for inhibiting T cell responses is the activity of ARG1 (11). CAT2 has been reported to modulate ARG1 activity in macrophages (24). Therefore, we investigated the possibility that CAT2 might be modulating ARG1 activity in MDSC. ARG1 catalyzes L-Arg to L-Ornithine and urea (11). Thus, we measured urea formation in $CAT2^{+/+}$ and $CAT2^{-/-}$MDSC to inspect the role of CAT2 in ARG1 activity. As expected, tumor MDSC had much greater ARG1 activity than bone marrow

$CD11b^{+}Gr\text{-}1^{+}$ cells. Importantly, the data demonstrate that ARG1 activity is comparable in $CAT2^{+/+}$ and $CAT2^{-/-}$MDSC (Fig. 5E). Next, we measured ARG1 protein levels in $CAT2^{+/+}$ and $CAT2^{-/-}$ tumor MDSC. In agreement with urea production observed, where L-Arg is supplied as a biochemical measure of relative ARG1 activity, we detected similar ARG1 protein levels in $CAT2^{+/+}$ and $CAT2^{-/-}$ MDSC (Fig. 5F).

To evaluate the contribution of NOS2 and ARG1 to MDSC suppressive function, we used NOS inhibitor, L-NMMA, and arginase inhibitor nor-NOHA. L-NMMA completely inhibited MDSC suppressive function. However, nor-NOHA had no effect on MDSC suppressive function (Fig. 5H). Thus, the data suggest that NOS2 metabolism is the major suppressive mechanism in MDSC from the RM1 ascites tumor model. These data suggest that the reduced NO production in $CAT2^{-/-}$MDSC accounts for the reduced suppressive capacity.

Elevated ROS production in $CAT2^{-/-}$ MDSC contributes to the suppressor activity

Although reduced, high levels of MDSC still possess suppressive ability in the absence of CAT2. Hence, we aimed to determine the mechanisms that regulate MDSC suppressive activity in a CAT2 independent manner. Previously L-Arg availability has been shown to modify NOS2 function such that when L-Arg is depleted in the local environment, NOS2 produces mostly $\cdot O_2^-$ instead of NO (25). $\cdot O_2^-$ can react with other molecules, such as H_2O and NO, and produce reactive oxygen species (ROS), thereby suppressing T cells (26). Therefore, we asked if KO MDSC had higher levels of ROS production. We measured ROS levels in WT and KO MDSC by DCFDA staining and found that KO MDSC had significantly higher ROS levels compared to WT MDSC (Fig. 6A). DCFDA staining of MDSC subsets revealed that ROS production in M-MDSC was similar in the absence or presence of CAT2 and the differential ROS production could be attributed to G-MDSC (Fig. 6B).

Next, we investigated the role of ROS formation in regulating MDSC suppressive function. We hypothesized that due to enhanced levels of production, in KO MDSC ROS plays a greater role in suppressive activity compared to WT MDSC. To this end, we used ROS inhibitor *N*-acetyl-L-cysteine (NAC) to assess the role of ROS in the suppressive function. Since $CAT2^{-/-}$ MDSC have low inhibitory activity, we used a high MDSC:OTI ratio (2:1) in the suppression assay to capture the expected reductions in suppressor activity due to the inhibition of ROS. As expected, NAC greatly reduced the suppressive capacity of KO MDSC, however it had no effect on WT MDSC (Fig. 6C). Since ROS were previously shown to mediate the suppressive function of MDSC (26), we concluded that the reason NAC did not affect suppressive activity of WT MDSC was due to the high MDSC:OTI ratio in the suppression assay. To address this, we co-cultured WT MDSC at differing ratios with OTI cells and determined the suppressive activity in the absence or presence of NAC. The results showed that at lower MDSC:OTI ratios ROS contributes to the suppressive activity of WT MDSC (Fig. 6D). Together, these data suggest that ROS production can mediate MDSC suppressive activity in a CAT2 independent manner and its role is enhanced in KO MDSC due to the elevated levels.

CAT2$^{-/-}$ MDSC display diminished capacity for controlling T-cell immunity *in vivo*

To evaluate whether CAT2 can modulate MDSC regulatory functions *in vivo* we performed a Winn assay, in which 3× 10^6 EG7 lymphoma cells were injected intradermally with or without activated OTI cells (27) in the presence or absence of MDSC. EG7 express ovalbumin and hence are susceptible to killing by OTI cells. EG7 tumors when implanted alone grew progressively. The presence of 10^4 OTI was sufficient to block tumor growth. In the presence of WT MDSC, OTI cells did not significantly inhibit tumor growth and, although slower, tumors grew progressively (Fig. 7A). To the contrary, the presence KO MDSC had no effect on OTI function (Fig. 7A). We further analyzed the role of CAT2 *in vivo* using another tumor model that allowed us to investigate CAT2-mediated effects on the regulatory function of endogenous tumor-induced MDSC. We implanted 3× 10^6 EG7 lymphoma cells intradermally into WT and KO mice. 7 days after injection, we adoptively transferred 1× 10^6activated OTI intravenously and monitored tumor growth. Tumor growth was slower in KO mice (Fig. 7B). Accordingly, we observed significantly slower tumor progression in KO mice when EG7 tumors were implanted subcutaneously (Supp. Figure 4). Together, these observations suggest that the ability of MDSC to regulate effector T cell function *in vivo* is impaired in the absence of CAT2.

Absence of CAT2 decreases the regulatory function of MDSC in an acute inflammation model

CAT2 is important in regulating MDSC function in a tumor-induced setting of chronic inflammation. In order to expand these findings to MDSC found in acute inflammatory sites, we utilized a prostate specific inflammation model, POET-3 (28). POET-3 express the chicken egg ovalbumin gene under the control of the prostate specific probasin promoter. Hence, adoptive transfer of ovalbumin specific T-cells (OTI) results in induction of prostate specific inflammation (28) with MDSC recruitment to prostate and spleen (Fig. 8A). MDSC isolated from prostate, but not from spleen, can suppress T-cell responses (22). We isolated CD11b$^+$Gr-1$^+$ cells from prostate and spleens of inflamed POET-3 mice and investigated *Cat2* expression levels. Similar to the results we obtained from the RM1 tumor model, *Cat2* is coordinately up-regulated with *Arg1* and *Nos2* in only MDSC isolated from prostate (Fig. 8B). To evaluate the role of CAT2 in MDSC in an acute inflammatory model, we bred our POET-3 mice with CAT2$^{-/-}$ mice. We investigated MDSC accumulation in CAT2 WT and KO POET-3 mice. Accumulation of both MDSC and MDSC subsets from the prostate and spleen were comparable between WT and KO POET-3 mice (not shown). Next, we evaluated if CAT2 modulated the suppressive capacity of MDSC. As seen in the tumor models, MDSC from acute inflammatory sites also had reduced suppressive capacity in the absence of CAT2 (Fig. 8C). Furthermore, we investigated if CAT2 was modulating MDSC regulatory function *in vivo*. Since the absence of CAT2 results in reduced MDSC function, we hypothesized that in KO POET-3 mice the ability of MDSC to inhibit T cells should be diminished, leading to a greater OTI population in the prostate. OTI cells express Thy1.1 and using this congenic marker we can monitor adoptively transferred OTI cells. We investigated the OTI population in prostate and spleens of WT and KO POET-3 mice. As expected, the KO POET-3 prostate had significantly more OTI cells, both as population percentages and absolute numbers (not shown). In order to ensure that the increase in OTI

cells in the KO POET-3 prostate was due to MDSC activity, we adoptively transferred WT MDSC into KO POET-3 mice. It was previously shown that culturing bone marrow cells with GM-CSF and IL-6 expand the $CD11b^{+}Gr\text{-}1^{+}$ population (9, 29). We isolated bone marrow from naive WT and KO mice and cultured the cells for 5 days with GM-CSF and IL-6. Then we transferred these *in vitro* generated KO MDSC into KO POET-3 and WT MDSC into WT or KO POET-3. As expected, the OTI population in the KO POET-3 was significantly greater than in WT POET-3 prostates. Adoptive transfer of WT MDSC into KO POET-3 could partially rescue this phenotype (Fig. 8D). Only MDSC in the prostate, but not the spleen, have suppressive function, therefore, MDSC in the spleen should not regulate OTI cells. As expected, WT and KO POET-3 have comparable OTI numbers in the spleens (Fig. 8E). In addition, we investigated IFN-γ formation in OTI cells from WT and KO POET-3. OTI isolated from the prostates of KO POET-3 trend toward higher levels of IFN-γ (Fig. 8F). OTI cells from the spleen displayed similar IFN-γ levels in WT and KO POET-3 mice (Fig. 8G).

In summary, these data suggest that elevated CAT2 expression is a marker of MDSC that acquired suppressive function, unlike those in spleen or bone marrow. CAT2 regulates MDSC suppressive capacity and is important for MDSC to have complete regulatory control of T-cell immunity.

Discussion

Myeloid derived suppressor cells are one of the dominant immunosuppressive populations that are present in the tumor microenvironment, impairing T cell function and promoting tumor progression (30). Therefore, MDSC present a major obstacle for the success of cancer immunotherapy. As a result, blocking MDSC function has been an attractive endeavor to complement cancer therapies. Indeed several studies demonstrated that depletion of MDSC or inhibiting MDSC function impaired cancer progression (31, 32). Although these studies are very promising, more specific strategies to block MDSC suppressive function are needed.

MDSC mediate their inhibitory effects on T cells through diverse mechanisms (33). One mechanism is the metabolism of amino acids by MDSC (34). For example, MDSC express enzymes that metabolize L-Arginine, L-Trytophan and cysteine, leading to their consumption from the microenvironment. Depletion of these amino acids results in T cell dysfunction (35-37). Additionally, MDSC can metabolize L-Arginine and L-Phenylalanine and generate end products that block T cell activities (38, 39). Among these, L-Arginine metabolism is considered to be the hallmark mechanism for MDSC-mediated T cell inhibition (11). Therefore, in this study we focused on the mechanism and functional impact of L-Arg uptake on MDSC. We postulated that we could control MDSC activity by modulating L-Arg entry into cells. L-Arg transport is mediated by y^{+}, $y^{+}L$ and $b^{0,+}$, $B^{0,+}$systems (13). The y^{+} system member CAT2 was shown to be the dominant L-Arg transporter in macrophages and was indirectly implicated as a transporter in MDSC (12). However, studies defining CAT2 as an L-Arg transporter and evaluation of the functional impact of CAT2 on MDSC function are lacking. Therefore, we initiated studies to define the role of CAT2 in MDSC.

Our data demonstrate that *Cat2* expression is induced in CD11b^{+}Gr-1^{+}cells only when they are exposed to activating cytokines *in vitro*. *In vivo*, only MDSC that reside at inflammatory or tumor sites, but not at peripheral sites, have elevated *Cat2* expression. In addition, *Cat2* induction is coordinately expressed with *Nos2* and *Arg1*. Notably, the data reported herein show that MDSC regulation of T cell immunity is compromised in the absence of CAT2, leading to inhibition of tumor growth. Thus *Cat2* may be useful in defining the functional state of CD11b^{+}Gr-1^{+} cells and serving as a target for regulating MDSC function.

Increased NOS2 and ARG1 activities are suggested to necessitate elevated L-Arg uptake in MDSC (30). We hypothesized that transportation through CAT2 is responsible for elevated L-Arg uptake in MDSC since its expression is coordinately induced with *Nos2* and *Arg1*. By comparing L-^{3}[H]-Arg incorporation in *Cat2*$^{+/+}$ and *Cat2*$^{-/-}$ MDSC, we showed that unlike macrophages where CAT2 is responsible for 90% of L-Arg transport, CAT2 mediates only ∼20% of L-Arg transport in MDSC. These data suggested that other L-Arg transport mechanisms compensate for the loss of CAT2. Evaluation of the contribution of other known L-Arg transporters showed that no members of b$^{0,+}$ or B$^{0,+}$ were expressed in MDSC. To further verify these results, we blocked the transport through b$^{0,+}$ or B$^{0,+}$ systems in MDSC and did not observe any alterations in L-Arg uptake (data not shown). These results are similar to Martin *et al.*'s findings that b$^{0,+}$ or B$^{0,+}$ systems do not contribute to L-Arg transport in bone marrow derived macrophages (17). We also investigated the participation of y^{+}L system in L-Arg transport in MDSC and found that transport through the y^{+}L system accounts for ∼25% of total transport. It is reported that in bone marrow cells in addition to carrier-mediated transport through y^{+} and y^{+}L systems, L-Arg can be taken up into cells by basal diffusion (17, 40). Indeed, we observed that a component of L-Arg uptake in MDSC could not be blocked by addition of saturating levels of non-radioactive L-Arg in transportation assays (not shown). Therefore, it is likely that in MDSC, basal diffusion or an unidentified L-Arg carrier is responsible for they^{+} and y^{+}L independent L-Arg transport. Additionally, we observed that L-Arg uptake was ∼10-fold higher in activated macrophages compared to MDSC. Comparative qPCR analysis revealed that macrophages had higher *Cat2* expression than MDSC (not shown). Although this observation might explain why macrophages have higher L-Arg uptake than MDSC, it is previously reported that mRNA levels of CATs do not necessarily reflect protein levels (14). Therefore, it is possible that the increase in *Cat2* gene expression in MDSC may not correlate with the functional protein levels. Unfortunately, due to lack of availability of specific antibodies we could not monitor CAT2 protein levels. Despite the compelling differences in L-Arg uptake through CAT2, NO production between MDSC and macrophages was altered in an equivalent manner in the absence of CAT2 (∼70% for each cell type). One possible explanation for these observations is that L-Arg compartmentalization might vary between the two cell types. It is proposed that there are distinct L-Arg pools inside the cells and the access of NOS2 to distinct pools might differ between different cell types (14, 41).

Importantly, our data revealed that CAT2 expression in MDSC regulates suppressive function. In the absence of CAT2, MDSC have lower suppressive activity due to lower production of NO. Since NOS2 expression is not modulated by CAT2, reduced NO levels in*Cat2*$^{-/-}$ MDSC is likely to be related to lower substrate availability. Similar to NOS2,

ARG1 expression is also independent of CAT2 and in an arginase functional assay, *Cat2*$^{+/+}$ and *Cat2*$^{-/-}$ MDSC displayed comparable arginase activity. This observation differs from a previous report that shows CAT2 deficiency enhances the activity of arginase in alternatively-activated macrophages (24). Given the differences reported herein between MDSC and macrophages regarding CAT2 expression and CAT2-mediated L-Arg transport, it is possible that CAT2-dependent modulation of ARG1 activity also varies between the two cell types. Also, it is important to stress that unlike in the Griess reaction, in this urea detection assay we lyse the MDSC and supply extracellular L-Arg for ARG1 enzyme to use. Hence, this assay measures the capacity of the enzyme to catalyze L-Arg, it does not reflect the intracellular activity of ARG1 in intact MDSC in the absence or presence of CAT2. We anticipate that in *Cat2*$^{-/-}$ MDSC, like NOS2, ARG1 activity is also reduced since CAT2 mediates its effects by controlling the substrate availability.

To further characterize CAT2-mediated MDSC suppressive function we investigated the role of previously described MDSC suppressive mechanisms. Inhibitor studies suggested that in the RM1 ascites model MDSC activity is mainly mediated through NOS2 activity. NOS inhibitor L-NMMA completely abrogated the suppressive function in MDSC even at high MDSC:OTI ratios, whereas the arginase inhibitor, nor-NOHA, had no effect. This observation might be linked to the suppression assay used, where MDSC and OTI are engaged in cell-to-cell contact to monitor antigen specific stimulation of OTI. Unlike NOS2, ARG1-mediated MDSC suppressive mechanisms have been reported to be independent of cell-to-cell contact (12, 42). In support of these results, Raber *et al*. also showed that in a suppression assay, where MDSC are in direct contact with T cells, L-NMMA completely blocked MDSC suppressive effect, while nor-NOHA had no effect (10). Although L-NMMA further inhibited the already reduced suppressive effect of *Cat2*$^{-/-}$ MDSC, we still detected residual suppressive activity, unlike *Cat2*$^{+/+}$ MDSC. It was reported previously that L-NMMA is transported through the y^+ system and has the same affinity for transporters as L-Arg (43). Therefore, it is likely that L-NMMA uptake in CAT2 ablated MDSC is lower and may be insufficient to completely block suppressive activity. Alternatively, this result may suggest that *Cat2*$^{-/-}$ MDSC utilizes NO-independent mechanisms to mediate T cell suppression. Because NOS2 in L-Arg depleted macrophages produce $\cdot O_2^-$ rather than the common product NO (25) and ROS formation is a suppressive mechanism of MDSC (26, 44), we evaluated ROS formation in MDSC. Indeed, we detected elevated levels of ROS in *Cat2*$^{-/-}$ MDSC. Inhibition of ROS resulted in greater changes in suppressive activity of *Cat2*$^{-/-}$ MDSC than *Cat2*$^{+/+}$ MDSC. ROS could mediate suppressive activity of WT MDSC only at low MDSC:OTI ratios. Overall, our data indicate that reduced suppressive capacity of *Cat2*$^{-/-}$ MDSC is due to lower NO production. *Cat2*$^{-/-}$ MDSC depend more on ROS to suppress T cells than *Cat2*$^{+/+}$ MDSC and ROS-mediated suppression, at least in part, account for the residual suppression in *Cat2*$^{-/-}$ MDSC. More studies are needed to investigate other CAT2 related suppressive mechanisms.

We also demonstrated that CAT2 is an important mediator of MDSC regulatory functions using *in vivo* models of acute inflammation and tumor formation. In the prostate specific inflammation model (POET-3), in the absence of CAT2, adoptively transferred OTI cells displayed enhanced expansion and higher frequency of IFN-γ producing cells in the prostate.

No differences were observed in splenic OTI cells, which is consistent with their activation state. These results are in accordance with our previous findings that showed when MDSC function is blocked by anti-Gr-1 during acute prostate inflammation, OTI proliferation and function is enhanced in the prostate, but not in the spleen (22). By controlling T-cell function MDSC promote tumor progression, so ablation of CAT2 in MDSC is expected to slow down tumor growth. In order to determine the effects of CAT2-mediated MDSC suppressive activity on tumor growth, we adopted an EG7 immunotherapy model (27). We implanted EG7 cells into *Cat2*$^{+/+}$ and *Cat2*$^{-/-}$ mice intradermally or subcutaneously and after 7 days we injected activated OTI cells intravenously. In *Cat2*$^{-/-}$ mice tumor growth was slower compared to *Cat2*$^{+/+}$ mice. These observations, together with results from the Winn assay, indicate that *Cat2*$^{-/-}$ MDSC have diminished capacity to control antitumor T cell responses. However, it is important to mention that in the absence of OTI transfer, EG7 growth was not significantly different between *Cat2*$^{+/+}$ and *Cat2*$^{-/-}$ mice. In fact, tumor growth rate was comparable also in EL4, MB49 and RM1 tumor models (not shown). CAT2 is an important regulator for other cell types as well, including macrophages and T cells (45, 46). The reason that tumor growth in *Cat2*$^{-/-}$ mice is not slower is most likely because of the CAT2 related deficiencies in other cell types, especially T cells. *Cat2* is expressed in activated T cells (46, 47) and L-Arg is essential for T cell functions (48, 49). Further studies are needed to elucidate the CAT2-dependent regulatory functions of multiple populations present in the tumor microenvironment.

Together, our findings describe the contribution of different L-Arg transportation systems in MDSC and define CAT2 as a major transporter that is induced in MDSC with immediate suppressor function. Therefore, CAT2 is a marker for functionally active MDSC. In addition, we demonstrate that CAT2 is a novel molecule mediating MDSC suppressive function and causing diminished antitumor immune responses. Hence, CAT2 may be utilized as a target to modulate MDSC activity in inflammatory diseases.

Supplementary Material

Refer to Web version on PubMed Central for supplementary material.

Acknowledgments

We thank Drs. Jeff Woodliff and Jill Hutchcroft at Purdue Flow Cytometry & Cell Separation Facility for cell sorting.

This work was supported by grants from NIDDK (DK084454), the NCI (CA173918), Purdue Center of Cancer Research P30 CA023168 and K22 CA118182.

References

1. Gabrilovich DI, Nagaraj S. Myeloid-derived suppressor cells as regulators of the immune system. Nature reviews Immunology. 2009; 9:162–174.
2. Casbon AJ, Reynaud D, Park C, Khuc E, Gan DD, Schepers K, Passegue E, Werb Z. Invasive breast cancer reprograms early myeloid differentiation in the bone marrow to generate immunosuppressive neutrophils. Proceedings of the National Academy of Sciences of the United States of America. 2015; 112:E566–575. [PubMed: 25624500]

3. Walter S, Weinschenk T, Stenzl A, Zdrojowy R, Pluzanska A, Szczylik C, Staehler M, Brugger W, Dietrich PY, Mendrzyk R, Hilf N, Schoor O, Fritsche J, Mahr A, Maurer D, Vass V, Trautwein C, Lewandrowski P, Flohr C, Pohla H, Stanczak JJ, Bronte V, Mandruzzato S, Biedermann T, Pawelec G, Derhovanessian E, Yamagishi H, Miki T, Hongo F, Takaha N, Hirakawa K, Tanaka H, Stevanovic S, Frisch J, Mayer-Mokler A, Kirner A, Rammensee HG, Reinhardt C, Singh-Jasuja H. Multipeptide immune response to cancer vaccine IMA901 after single-dose cyclophosphamide associates with longer patient survival. Nature medicine. 2012; 18:1254–1261.

4. Gabitass RF, Annels NE, Stocken DD, Pandha HA, Middleton GW. Elevated myeloid-derived suppressor cells in pancreatic, esophageal and gastric cancer are an independent prognostic factor and are associated with significant elevation of the Th2 cytokine interleukin-13. Cancer immunology, immunotherapy : CII. 2011; 60:1419–1430. [PubMed: 21644036]

5. Wesolowski R, Markowitz J, Carson WE 3rd. Myeloid derived suppressor cells - a new therapeutic target in the treatment of cancer. Journal for immunotherapy of cancer. 2013; 1:10. [PubMed: 24829747]

6. Haile LA, von Wasielewski R, Gamrekelashvili J, Kruger C, Bachmann O, Westendorf AM, Buer J, Liblau R, Manns MP, Korangy F, Greten TF. Myeloid-derived suppressor cells in inflammatory bowel disease: a new immunoregulatory pathway. Gastroenterology. 2008; 135:871–881. 881.e871–875. [PubMed: 18674538]

7. Zhu B, Bando Y, Xiao S, Yang K, Anderson AC, Kuchroo VK, Khoury SJ. CD11b+Ly-6C(hi) suppressive monocytes in experimental autoimmune encephalomyelitis. Journal of immunology (Baltimore, Md : 1950). 2007; 179:5228–5237.

8. Fujii W, Ashihara E, Hirai H, Nagahara H, Kajitani N, Fujioka K, Murakami K, Seno T, Yamamoto A, Ishino H, Kohno M, Maekawa T, Kawahito Y. Myeloid-derived suppressor cells play crucial roles in the regulation of mouse collagen-induced arthritis. Journal of immunology (Baltimore, Md : 1950). 2013; 191:1073–1081.

9. Haverkamp JM, Smith AM, Weinlich R, Dillon CP, Qualls JE, Neale G, Koss B, Kim Y, Bronte V, Herold MJ, Green DR, Opferman JT, Murray PJ. Myeloid-derived suppressor activity is mediated by monocytic lineages maintained by continuous inhibition of extrinsic and intrinsic death pathways. Immunity. 2014; 41:947–959. [PubMed: 25500368]

10. Raber PL, Thevenot P, Sierra R, Wyczechowska D, Halle D, Ramirez ME, Ochoa AC, Fletcher M, Velasco C, Wilk A, Reiss K, Rodriguez PC. Subpopulations of myeloid-derived suppressor cells impair T cell responses through independent nitric oxide-related pathways. International journal of cancer Journal international du cancer. 2014; 134:2853–2864. [PubMed: 24259296]

11. Bronte V, Zanovello P. Regulation of immune responses by L-arginine metabolism. Nature reviews Immunology. 2005; 5:641–654.

12. Raber P, Ochoa AC, Rodriguez PC. Metabolism of L-arginine by myeloid-derived suppressor cells in cancer: mechanisms of T cell suppression and therapeutic perspectives. Immunological investigations. 2012; 41:614–634. [PubMed: 23017138]

13. Deves R, Boyd CA. Transporters for cationic amino acids in animal cells: discovery, structure, and function. Physiological reviews. 1998; 78:487–545. [PubMed: 9562037]

14. Closs EI, Simon A, Vekony N, Rotmann A. Plasma membrane transporters for arginine. The Journal of nutrition. 2004; 134:2752S–2759S. discussion 2765S-2767S. [PubMed: 15465780]

15. Verrey F, Closs EI, Wagner CA, Palacin M, Endou H, Kanai Y. CATs and HATs: the SLC7 family of amino acid transporters. Pflugers Archiv : European journal of physiology. 2004; 447:532–542. [PubMed: 14770310]

16. Nicholson B, Manner CK, Kleeman J, MacLeod CL. Sustained nitric oxide production in macrophages requires the arginine transporter CAT2. The Journal of biological chemistry. 2001; 276:15881–15885. [PubMed: 11278602]

17. Martin L, Comalada M, Marti L, Closs EI, MacLeod CL, Martin del Rio R, Zorzano A, Modolell M, Celada A, Palacin M, Bertran J. Granulocyte-macrophage colony-stimulating factor increases L-arginine transport through the induction of CAT2 in bone marrow-derived macrophages. American journal of physiology Cell physiology. 2006; 290:C1364–1372. [PubMed: 16371438]

18. Rodriguez PC, Quiceno DG, Zabaleta J, Ortiz B, Zea AH, Piazuelo MB, Delgado A, Correa P, Brayer J, Sotomayor EM, Antonia S, Ochoa JB, Ochoa AC. Arginase I production in the tumor

microenvironment by mature myeloid cells inhibits T-cell receptor expression and antigen-specific T-cell responses. Cancer research. 2004; 64:5839–5849. [PubMed: 15313928]

19. Lees JR, Charbonneau B, Hayball JD, Diener K, Brown M, Matusik R, Cohen MB, Ratliff TL. T-cell recognition of a prostate specific antigen is not sufficient to induce prostate tissue destruction. The Prostate. 2006; 66:578–590. [PubMed: 16388504]
20. Qualls JE, Subramanian C, Rafi W, Smith AM, Balouzian L, DeFreitas AA, Shirey KA, Reutterer B, Kernbauer E, Stockinger S, Decker T, Miyairi I, Vogel SN, Salgame P, Rock CO, Murray PJ. Sustained generation of nitric oxide and control of mycobacterial infection requires argininosuccinate synthase 1. Cell Host Microbe. 2012; 12:313–323. [PubMed: 22980328]
21. Gallina G, Dolcetti L, Serafini P, De Santo C, Marigo I, Colombo MP, Basso G, Brombacher F, Borrello I, Zanovello P, Bicciato S, Bronte V. Tumors induce a subset of inflammatory monocytes with immunosuppressive activity on CD8+ T cells. The Journal of clinical investigation. 2006; 116:2777–2790. [PubMed: 17016559]
22. Haverkamp JM, Crist SA, Elzey BD, Cimen C, Ratliff TL. In vivo suppressive function of myeloid-derived suppressor cells is limited to the inflammatory site. European journal of immunology. 2011; 41:749–759. [PubMed: 21287554]
23. Corzo CA, Condamine T, Lu L, Cotter MJ, Youn JI, Cheng P, Cho HI, Celis E, Quiceno DG, Padhya T, McCaffrey TV, McCaffrey JC, Gabrilovich DI. HIF-1alpha regulates function and differentiation of myeloid-derived suppressor cells in the tumor microenvironment. The Journal of experimental medicine. 2010; 207:2439–2453. [PubMed: 20876310]
24. Thompson RW, Pesce JT, Ramalingam T, Wilson MS, White S, Cheever AW, Ricklefs SM, Porcella SF, Li L, Ellies LG, Wynn TA. Cationic amino acid transporter-2 regulates immunity by modulating arginase activity. PLoS pathogens. 2008; 4:e1000023. [PubMed: 18369473]
25. Xia Y, Zweier JL. Superoxide and peroxynitrite generation from inducible nitric oxide synthase in macrophages. Proceedings of the National Academy of Sciences of the United States of America. 1997; 94:6954–6958. [PubMed: 9192673]
26. Corzo CA, Cotter MJ, Cheng P, Cheng F, Kusmartsev S, Sotomayor E, Padhya T, McCaffrey TV, McCaffrey JC, Gabrilovich DI. Mechanism regulating reactive oxygen species in tumor-induced myeloid-derived suppressor cells. Journal of immunology (Baltimore, Md : 1950). 2009; 182:5693–5701.
27. Helmich BK, Dutton RW. The role of adoptively transferred CD8 T cells and host cells in the control of the growth of the EG7 thymoma: factors that determine the relative effectiveness and homing properties of Tc1 and Tc2 effectors. Journal of immunology (Baltimore, Md : 1950). 2001; 166:6500–6508.
28. Haverkamp JM, Charbonneau B, Crist SA, Meyerholz DK, Cohen MB, Snyder PW, Svensson RU, Henry MD, Wang HH, Ratliff TL. An inducible model of abacterial prostatitis induces antigen specific inflammatory and proliferative changes in the murine prostate. The Prostate. 2011; 71:1139–1150. [PubMed: 21656824]
29. Marigo I, Bosio E, Solito S, Mesa C, Fernandez A, Dolcetti L, Ugel S, Sonda N, Bicciato S, Falisi E, Calabrese F, Basso G, Zanovello P, Cozzi E, Mandruzzato S, Bronte V. Tumor-induced tolerance and immune suppression depend on the C/EBPbeta transcription factor. Immunity. 2010; 32:790–802. [PubMed: 20605485]
30. Ostrand-Rosenberg S. Myeloid-derived suppressor cells: more mechanisms for inhibiting antitumor immunity. Cancer immunology, immunotherapy : CII. 2010; 59:1593–1600. [PubMed: 20414655]
31. Iclozan C, Antonia S, Chiappori A, Chen DT, Gabrilovich D. Therapeutic regulation of myeloid-derived suppressor cells and immune response to cancer vaccine in patients with extensive stage small cell lung cancer. Cancer immunology, immunotherapy : CII. 2013; 62:909–918. [PubMed: 23589106]
32. Highfill SL, Cui Y, Giles AJ, Smith JP, Zhang H, Morse E, Kaplan RN, Mackall CL. Disruption of CXCR2-mediated MDSC tumor trafficking enhances anti-PD1 efficacy. Science translational medicine. 2014; 6:237ra267.
33. Ostrand-Rosenberg S, Sinha P. Myeloid-derived suppressor cells: linking inflammation and cancer. J Immunol. 2009; 182:4499–4506. [PubMed: 19342621]

34. Marigo I, Dolcetti L, Serafini P, Zanovello P, Bronte V. Tumor-induced tolerance and immune suppression by myeloid derived suppressor cells. Immunol Rev. 2008; 222:162–179. [PubMed: 18364001]
35. Fallarino F, Grohmann U, You S, McGrath BC, Cavener DR, Vacca C, Orabona C, Bianchi R, Belladonna ML, Volpi C, Santamaria P, Fioretti MC, Puccetti P. The combined effects of tryptophan starvation and tryptophan catabolites down-regulate T cell receptor zeta-chain and induce a regulatory phenotype in naive T cells. J Immunol. 2006; 176:6752–6761. [PubMed: 16709834]
36. Rodriguez PC, Zea AH, DeSalvo J, Culotta KS, Zabaleta J, Quiceno DG, Ochoa JB, Ochoa AC. L-arginine consumption by macrophages modulates the expression of CD3 zeta chain in T lymphocytes. J Immunol. 2003; 171:1232–1239. [PubMed: 12874210]
37. Srivastava MK, Sinha P, Clements VK, Rodriguez P, Ostrand-Rosenberg S. Myeloid-derived suppressor cells inhibit T-cell activation by depleting cystine and cysteine. Cancer research. 2010; 70:68–77. [PubMed: 20028852]
38. Nagaraj S, Gupta K, Pisarev V, Kinarsky L, Sherman S, Kang L, Herber DL, Schneck J, Gabrilovich DI. Altered recognition of antigen is a mechanism of CD8+ T cell tolerance in cancer. Nat Med. 2007; 13:828–835. [PubMed: 17603493]
39. Boulland ML, Marquet J, Molinier-Frenkel V, Moller P, Guiter C, Lasoudris F, Copie-Bergman C, Baia M, Gaulard P, Leroy K, Castellano F. Human IL4I1 is a secreted L-phenylalanine oxidase expressed by mature dendritic cells that inhibits T-lymphocyte proliferation. Blood. 2007; 110:220–227. [PubMed: 17356132]
40. Speake PF, Glazier JD, Ayuk PTY, Reade M, Sibley CP, D'Souza SW. L-Arginine transport across the basal plasma membrane of the syncytiotrophoblast of the human placenta from normal and preeclamptic pregnancies. The Journal of clinical endocrinology and metabolism. 2003; 88:4287–4292. [PubMed: 12970300]
41. Closs EI, Scheld JS, Sharafi M, Forstermann U. Substrate supply for nitric-oxide synthase in macrophages and endothelial cells: role of cationic amino acid transporters. Molecular pharmacology. 2000; 57:68–74. [PubMed: 10617680]
42. Rodriguez PC, Ochoa AC. Arginine regulation by myeloid derived suppressor cells and tolerance in cancer: mechanisms and therapeutic perspectives. Immunol Rev. 2008; 222:180–191. [PubMed: 18364002]
43. Schmidt K, Klatt P, Mayer B. Characterization of endothelial cell amino acid transport systems involved in the actions of nitric oxide synthase inhibitors. Molecular pharmacology. 1993; 44:615–621. [PubMed: 7690451]
44. Kusmartsev S, Nefedova Y, Yoder D, Gabrilovich DI. Antigen-specific inhibition of CD8+ T cell response by immature myeloid cells in cancer is mediated by reactive oxygen species. Journal of immunology (Baltimore, Md: 1950). 2004; 172:989–999.
45. Ezernitchi AV, Vaknin I, Cohen-Daniel L, Levy O, Manaster E, Halabi A, Pikarsky E, Shapira L, Baniyash M. TCR zeta down-regulation under chronic inflammation is mediated by myeloid suppressor cells differentially distributed between various lymphatic organs. Journal of immunology (Baltimore, Md : 1950). 2006; 177:4763–4772.
46. MacLeod CL, Finley K, Kakuda D, Kozak CA, Wilkinson MF. Activated T cells express a novel gene on chromosome 8 that is closely related to the murine ecotropic retroviral receptor. Molecular and cellular biology. 1990; 10:3663–3674. [PubMed: 1694015]
47. Reizer J, Finley K, Kakuda D, MacLeod CL, Reizer A, Saier MH Jr. Mammalian integral membrane receptors are homologous to facilitators and antiporters of yeast, fungi, and eubacteria. Protein science : a publication of the Protein Society. 1993; 2:20–30. [PubMed: 8382989]
48. Rodriguez PC, Quiceno DG, Ochoa AC. L-arginine availability regulates T-lymphocyte cell-cycle progression. Blood. 2007; 109:1568–1573. [PubMed: 17023580]
49. Zea AH, Rodriguez PC, Culotta KS, Hernandez CP, DeSalvo J, Ochoa JB, Park HJ, Zabaleta J, Ochoa AC. L-Arginine modulates CD3zeta expression and T cell function in activated human T lymphocytes. Cellular immunology. 2004; 232:21–31. [PubMed: 15922712]

Abbreviations used in this paper

Arg1	arginase 1
Cat2	cationic amino acid transporter 2
G-MDSC	granulocytic myeloid derived suppressor cells
KO	Cat2 knock out mice
L-Arg	L-Arginine
L-Leu	L-Leucine
LNMMA	N^G-Monomethyl-L-arginine
MDSC	myeloid derived suppressor cells
M-MDSC	monocytic myeloid derived suppressor cells
NAC	*n*-acetyl-L-cysteine
NEM	*N*-ethyl maleimide
nor-NOHA	$N^{(\omega)}$-hydroxy-L-arginine
Nos2	Nitric oxide synthase 2
OTI	ovalbumin specific T cells
OVA	ovalbumin
POET-3	prostate ovalbumin expressing mice-3
ROS	reactive oxygen species
WT	wild type mice

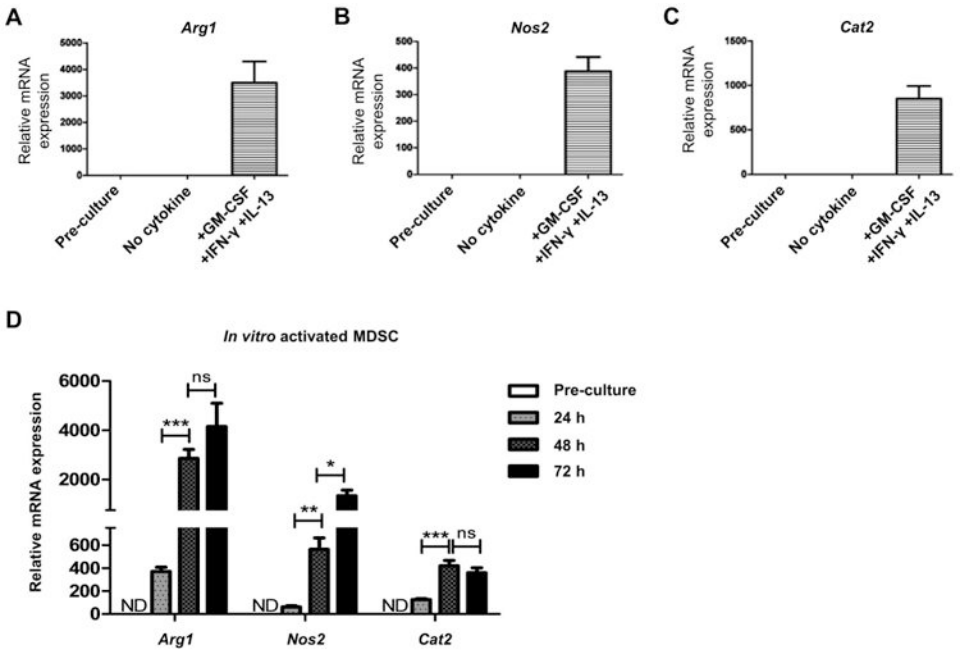

Figure 1.

Cat2 is coordinately induced with *Arg1* and *Nos2* in MDSC. $CD11b^{+}Gr\text{-}1^{+}$ cells were isolated from bone marrow of naïve wild type mice and cultured with or without GM-CSF, IL-13 and IFN- γ. mRNA was isolated after 3 days of culture **(A)** or every 24 hour during culture (n=4 mice, *** p=0.0005, ** p=0.0027, * p=0.0211, *** p=0.0009) **(B).** *Arg1*, *Nos2* and *Cat2* gene expression were analyzed by qPCR. Data are representative of at least 3 independent experiments. For all experiments errors bars indicate ±SEM.

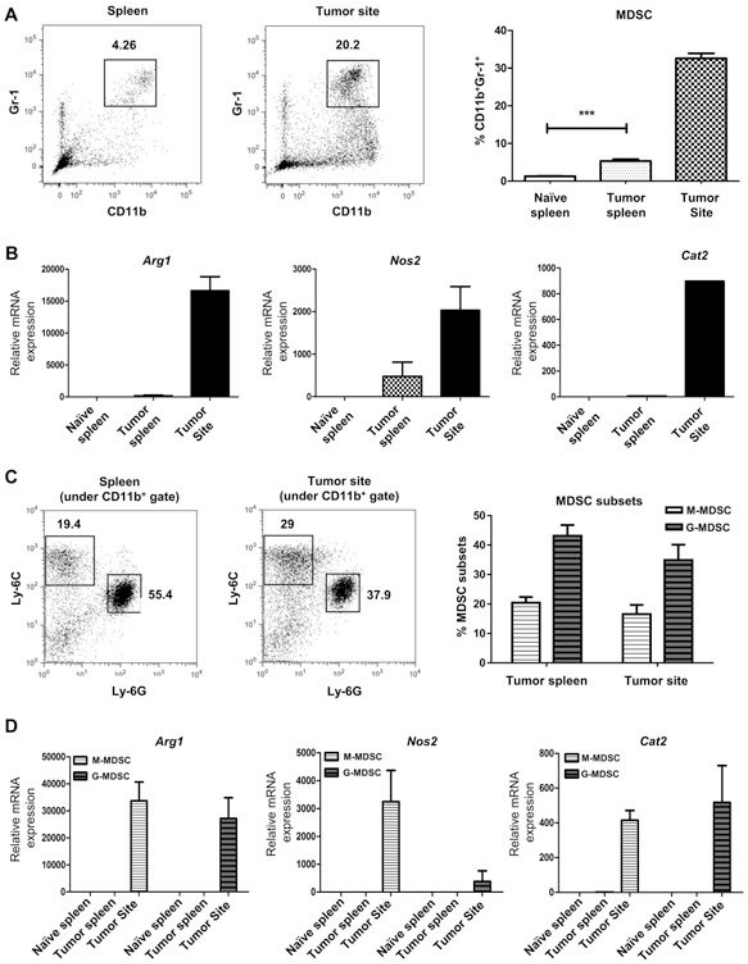

Figure 2.

Cat2 is induced in functionally active MDSC. $CD11b^{+}Gr\text{-}1^{+}$ and $CD11b^{+}Ly6C^{high}Ly6G^{-}$ (M-MDSC), $CD11b^{+}Ly6C^{low}Ly6G^{+}$ (G-MDSC) cells were isolated by FACS from ascites and spleen of RM1 i.p. tumor bearing $Cat2^{+/+}$ (WT) mice 6 days after tumor implantation or from the spleens of naïve mice. The percentage of $CD11b^{+}Gr\text{-}1^{+}$ cells were demonstrated under SSC/FSC gate (n=4, *** p=0.0002) **(A)**. Percentages of $CD11b^{+}Ly6C^{high}Ly6G^{-}$ (M-MDSC) and $CD11b^{+}Ly6C^{low}Ly6G^{+}$ (G-MDSC) were demonstrated under $CD11b^{+}$ gate. Data are pooled from 6 independent experiments **(C)**. mRNA was freshly isolated and analyzed by qPCR for *Arg1*, *Nos2* and *Cat2* expression **(B and D)**. Data are representative of at least 3 independent experiments. For all experiments errors bars indicate ±SEM.

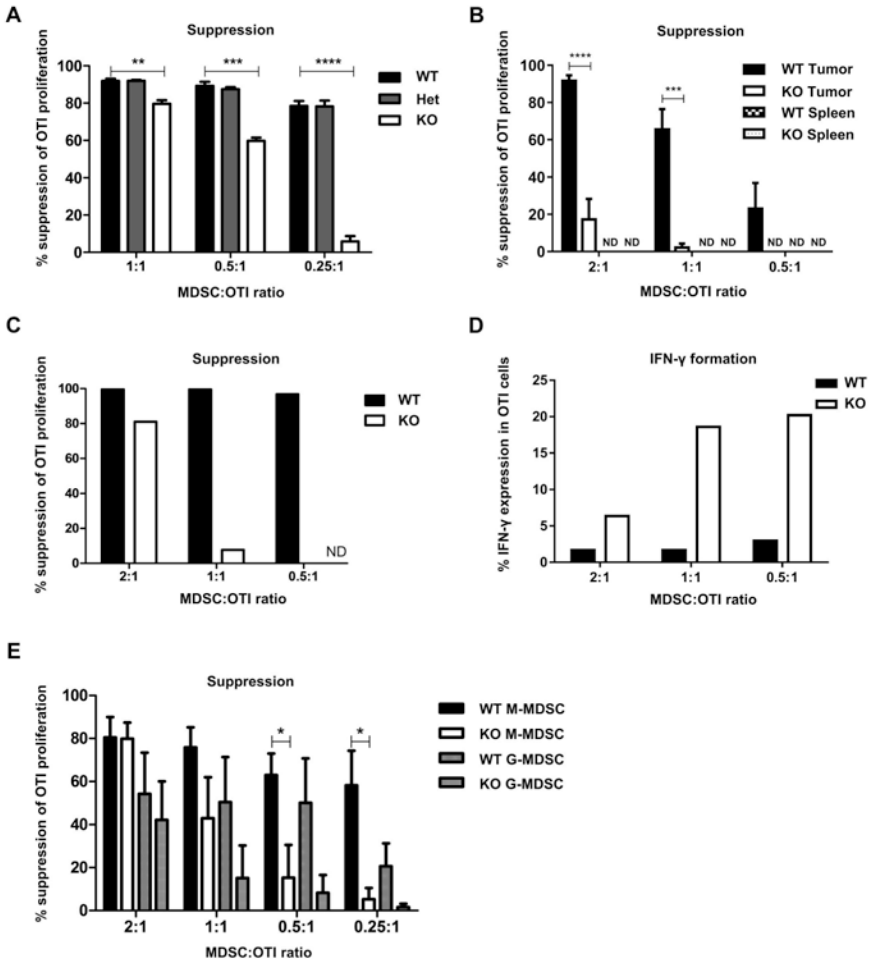

Figure 3.

MDSC suppressive capacity is reduced in the absence of CAT2. $CD11b^{+}Gr\text{-}1^{+}$ cells were isolated from bone marrow of naïve mice and cultured with GM-CSF, IL-13 and IFN- γ. After 3 days cells were harvested and co-cultured with naïve OTI in the presence of SIINFEKL at indicated ratios for another 3 days. BrdU was added 6 hours before harvest. OTI proliferation was evaluated by measuring BrdU incorporation. Data are representative of 3 independent experiments (n=3-4/group, ** p=0.0057, *** p=0.0001, **** p<0.0001) **(A)**. $CD11b^{+}Gr\text{-}1^{+}$ cells were isolated from tumor site and spleens of RM1 bearing WT and KO mice (n=3-5/group, pooled) 6 days after tumor implantation and co-cultured with preactivated OTIs for 18 hours. BrdU was added 6 hours before harvest. OTI proliferation was evaluated by measuring BrdU incorporation. Data are pooled from 5 and 3 independent experiments for tumor and for spleen, respectively (*** p=0.0002, **** p<0.0001) **(B)**. $CD11b^{+}Gr\text{-}1^{+}$ cells from the ascites of RM1 i.p. tumor bearing *Cat2*+/+ (WT) and $Cat2^{-/-}$ (KO) mice (n=5/group, pooled) were co-cultured with naive OTI cells with SIINFEKL for 48 hours. BrdU and protein transport inhibitor were added 6 hours before harvest. OTI proliferation was evaluated by measuring BrdU incorporation **(C)** IFN-γ levels in OT-I cells were determined by flow cytometry for intracellular IFN-γ staining **(D)**. Data are representative of 5 independent experiments. M-MDSC and G-MDSC were isolated by

FACS from the ascites of RM1 i.p. tumor bearing WT and KO mice (n=3-5/group, pooled) 6 days after tumor implantation **(E)** and co-cultured with naive OTI cells with SIINFEKL for 48-72 hours. BrdU was added 6 hours before harvest. OTI proliferation was evaluated by measuring BrdU incorporation. Data are pooled from 5 independent experiments (* p=0.0312 at 0.5:1 and 0.0139 at 0.25:1) **(F)**. For all experiments errors bars indicate ±SEM.

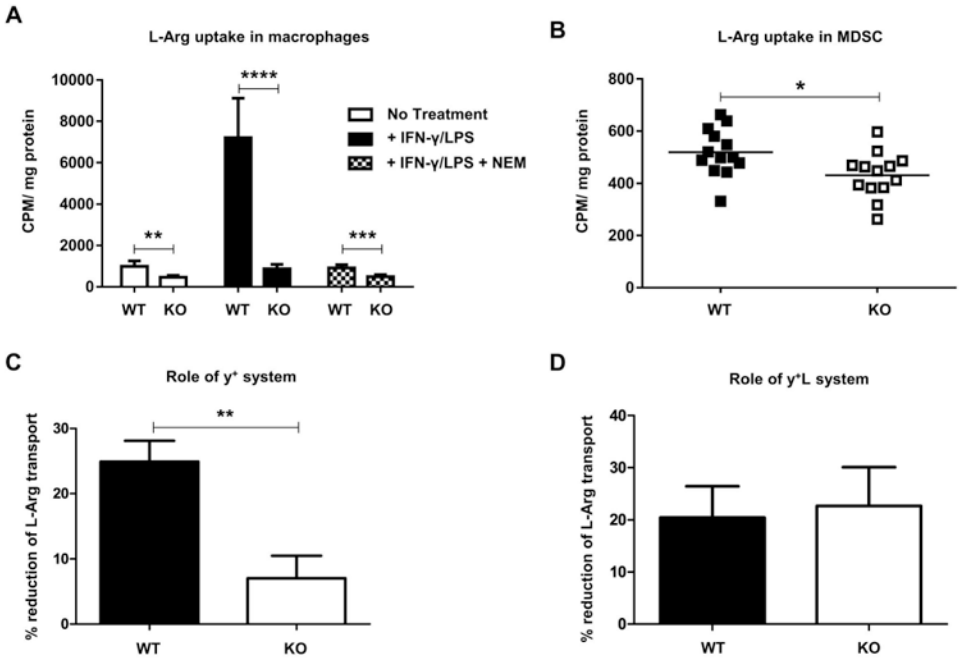

Figure 4.

CAT2 mediates L-Arginine transportation in MDSC. Thioglycollate elicited peritoneal macrophages from *Cat2*$^{+/+}$ (WT) and *Cat2*$^{-/-}$ (KO) mice (n=5/group) were activated with LPS and IFN-γ for 18h. L-Arginine transport was measured by using 6μCi/ml L-^{3}[H]-Arg in Na^{+} containing buffer. For *N*-ethyl maleimide (NEM), cells were pretreated with 5 mM NEM for 5 min and washed with transport buffer before measuring uptake. Data are representative of 3 independent experiments. (**** $p<0.0001$) **(A).** $CD11b^{+}Gr\text{-}1^{+}$ cells were isolated from ascites of RM1 tumor bearing WT and KO mice and cultured over night with GM-CSF, IL-13 and IFN- γ. Total L-Arginine transport was measured by using 6μCi/ml L-^{3}[H]-Arg in Na^{+} containing buffer. Data are pooled from 3 independent experiments. (n=13/group, * $p=0.0184$) **(B)** Data correspond to reduction of total L-^{3}[H]-Arg transport when y^{+} system was blocked using 5 mM NEM in WT and KO MDSC. Data are pooled from 3 independent experiments (n=10/group, ** $p=0.0016$) **(C)**. Data correspond to reduction of total L-^{3}[H]-Arg transport when y^{+}L system was blocked due to the presence of 5 mM L-Leu in transport media. Data are pooled from 4 independent experiments (n=13/group) **(D)**. All error bars indicate ±SEM.

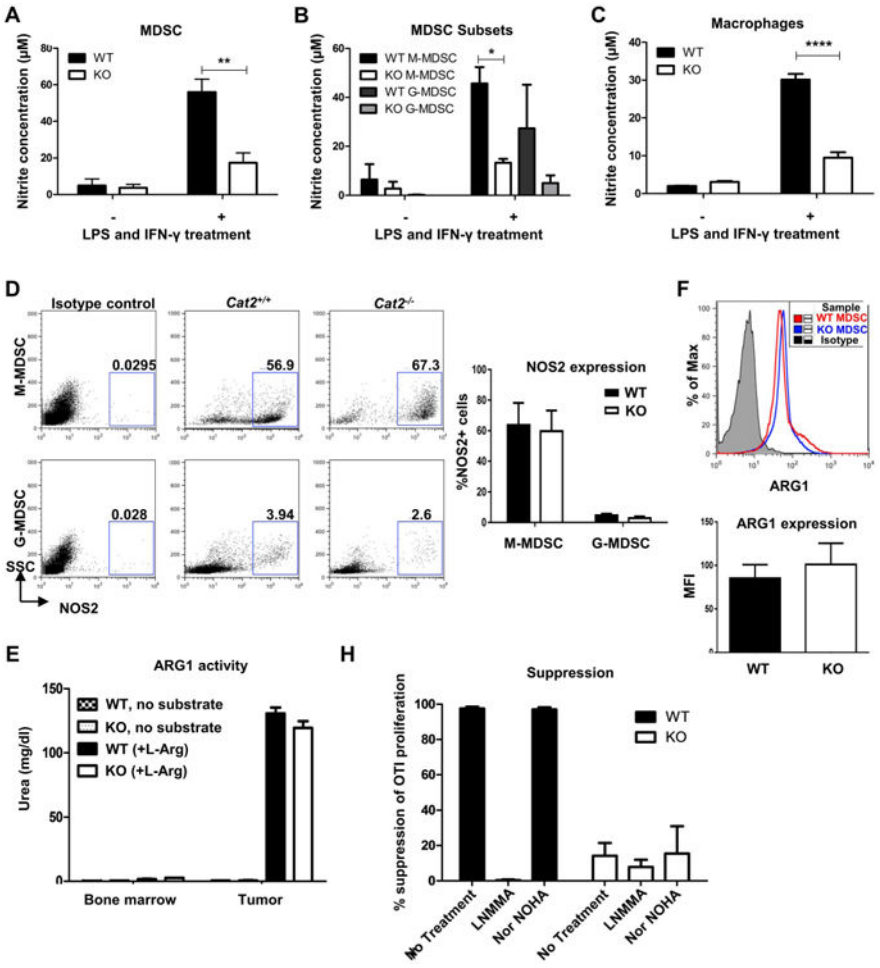

Figure 5.

Cat2$^{-/-}$ MDSC have reduced NO production. CD11b^{+}Gr-1^{+} MDSC **(A)** and CD11b^{+}LyC^{high}Ly6G^{-} (M-MDSC) and CD11b^{+}LyC^{low}Ly6G^{+} (G-MDSC) subsets **(B)** were isolated from tumor site of RM1 bearing *Cat2*$^{+/+}$ (WT) and *Cat2*$^{-/-}$ (KO) mice. Cells were cultured in the presence and absence of LPS and IFN-γ for 24 hours. Nitrite formation upon stimulation with LPS and IFN-γ was measured in a Griess Assay. Data are pooled from 2 independent experiments (n=5-9 mice/group for MDSC. ** p=0.0065, n=4/group, pooled for subsets. * p=0.0426). Thioglycollate elicited peritoneal macrophages from *Cat2*$^{+/+}$ (WT) and *Cat2*$^{-/-}$ (KO) mice (n=4/group) were activated with LPS and IFN-γ for 18h. Nitrite formation was measured in a Griess Assay. Data are representative of at least 2 independent experiments (**** p<0.0001) **(C)**. Cells from the ascites of WT and KO RM1 mice were cultured with LPS and IFN-γ overnight prior to intracellular staining of NOS2 for flow cytometry. Percentages of NOS2+ cells were demonstrated under CD11b^{+}LyC^{high}Ly6G^{-} (M-MDSC) and CD11b^{+}LyC^{low}Ly6G^{+} (G-MDSC) gates (n=4-5/group). Data are representative of 3 independently performed experiments **(D)**. Quantichrome Urea Assay Kit that measures urea and citrulline was utilized to measure arginase activity in CD11b^{+}Gr-1^{+} cells freshly isolated from the bone marrow and ascites of WT and KO RM1 mice (n=4/group) with or without supplementing L-Arg. Data are representative of 3 independent

experiments **(E)**. Cells freshly isolated from the ascites of WT and KO RM1 mice were stained with anti-ARG1 antibody. ARG1 expression was detected by flow cytometry. Mean fluorescent intensity (MFI) of ARG1 expression was reported under $CD11b^{+}Gr\text{-}1^{+}$ gate (n=4/group). Data are representative of 3 independently performed experiments **(F)**. WT and KO MDSC were used in a 48-hour suppression assay at 2:1 (MDSC:OTI) ratio in the presence or absence of NOS inhibitor, LNMMA (0.5 mM), ARG inhibitor, nor-NOHA (0.5 mM). BrdU was added 6 hours before harvest. OTI proliferation was evaluated by measuring BrdU incorporation. Data were pooled from 2 independent experiments **(H)**. For all experiments errors bars indicate ±SEM.

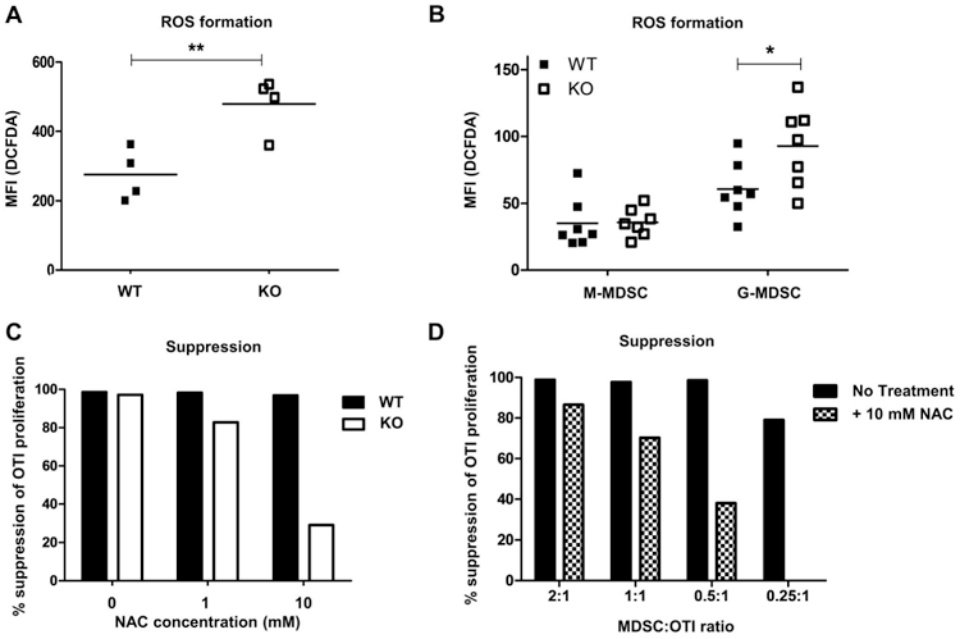

Figure 6.

Cat2$^{-/-}$ MDSC have increased ROS formation. Cells from ascites of i.p. RM1 bearing WT and KO mice were analyzed for ROS levels. DCFDA signal was analyzed under the gates for CD11b^{+}Gr-1^{+} (n=4/group)**(A)** and CD11b^{+}LyC^{high}Ly6G^{-} (M-MDSC) and CD11b^{+}LyC^{low}Ly6G^{+} (G-MDSC) subsets (n=8/group, data are pooled from 2 independent experiments) **(B)**. Signal intensity was represented as MFI. CD11b^{+}Gr-1^{+} cells were isolated by FACS from the ascites of RM1 i.p. tumor bearing *Cat2*$^{+/+}$ (WT) and *Cat2*$^{-/-}$ (KO) mice (n=5/group, pooled)6 days after tumor implantation and suppression assay was performed at 2:1 (MDSC:OTI) ratio in the presence of differing concentrations of ROS inhibitor, NAC **(C)**. WT MDSC were used for suppression assay at indicated MDSC:OTI ratios with or without 10 mM NAC **(D).** Data are representative of at least 2 independent experiments. All suppression assays were performed by co-culturing MDSC with preactivated OTI cells for 48 hours. BrdU was added 6 hours before harvest. OTI proliferation was evaluated by measuring BrdU incorporation. For all experiments errors bars indicate ±SEM.

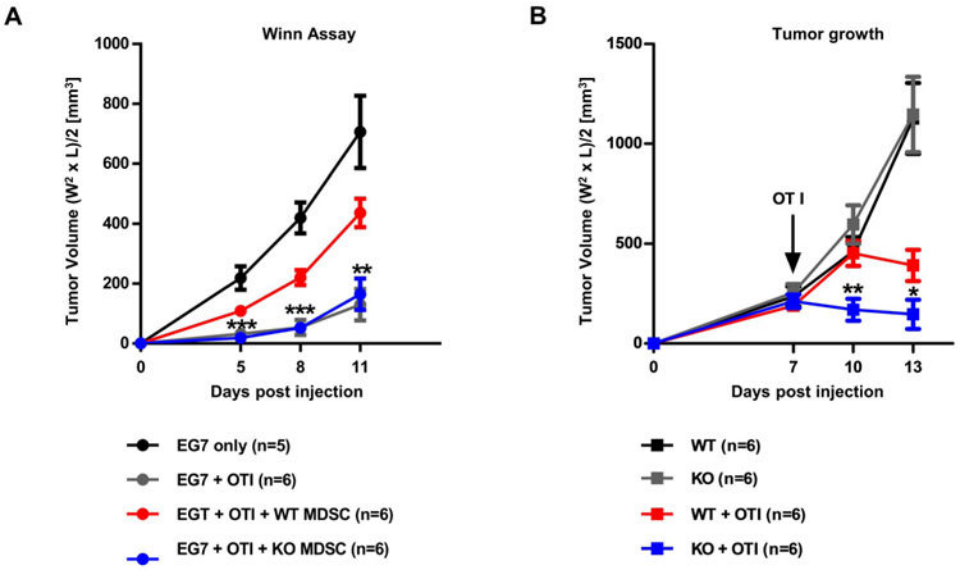

Figure 7.

CAT2$^{-/-}$ MDSC display diminished capacity for controlling T-cell immunity *in vivo*. *Cat2*$^{-/-}$ mice were injected intradermally with 3× 10^6 EG7 lymphoma cells alone, 3× 10^6 EG7 with 10^4 activated OTIs, 3× 10^6 EG7 with 10^4 activated OTIs and 10^4 *Cat2*$^{+/+}$ or *Cat2*$^{-/-}$ CD11b$^+$Gr-1$^+$ cells. Data are pooled from 2 independent experiments (n=5-6 mice/group). p values for the comparison of WT or KO MDSC received groups are 0.0001, 0.0003 and 0.0033 on Day 5, 8 and 11, respectively **(A)**. *Cat2*$^{+/+}$ and *Cat2*$^{-/-}$ mice were injected intradermally with 3× 10^6 EG7 lymphoma cells. 7 days after tumor inoculation, mice were intravenously injected with 10^6 activated OTI cells (n=6/group). Tumor growth was monitored. p values for the comparison of WT and KO mice that received OTI are 0.0072 and 0.0449 on Day 10 and 13, respectively. Tumor size was calculated as (W^2× L) /2 [mm^3]. Errors bars indicate ±SEM.

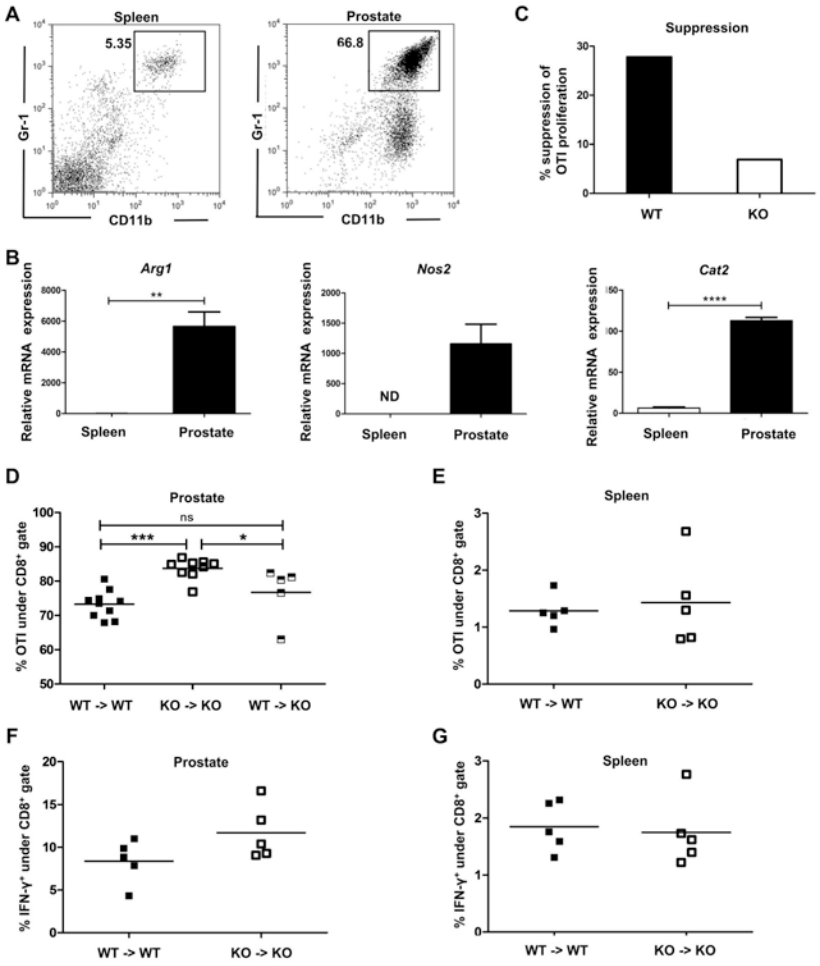

Figure 8.

CAT2 modulates MDSC regulatory functions in an acute prostate inflammation model.Prostate Ovalbumin Expressing Transgenic (POET-3) mice (n=3) were injected with 5×10^6 activated OTI cells to induce prostate inflammation. 5 days later spleen and prostate $CD11b^+Gr\text{-}1^+$ cells (under $CD45^+$ gate) **(A)** were sorted by FACS. mRNA was freshly isolated from sorted cells and analyzed by qPCR for *Arg1*, *Nos2* and *Cat2* expression **(B)**. Data are representative of at least 3 independent experiments (** p=0.038, **** p<0.0001). MDSC were isolated from inflamed prostates of $Cat2^{+/+}$ and $Cat2^{-/-}$ POET-3 mice. (n=3/group, pooled) and co-cultured with preactivated OTI cells for 48 hours. BrdU was added 6 hours before harvest. OTI proliferation was evaluated by measuring BrdU incorporation **(C)**. 5×10^6 activated OTI cells were intravenously injected into POET-3 mice to induce inflammation. 2 days later, mice were adoptively transferred (i.p.) with 4×10^6 $Cat2^{+/+}$ and $Cat2^{-/-}$ bone marrow cells that were cultured 5 days with GM-CSF and IL-6.$Cat2^{+/+}$ POET-3 received $Cat2^{+/+}$ cells and $Cat2^{-/-}$ POET-3 received $Cat2^{-/-}$ or $Cat2^{+/+}$ cells. Percentage of $Thy1.1^+$ (OTI) cells in 5-day inflamed POET-3 prostate **(D)** and spleen **(E)** are represented under $CD45^+CD8^+$ gate. Each individual datum point represents a single mouse (***p<0.001, *p<0.05). Prostate **(F)** and spleen **(G)** cells were cultured with SIINFEKL and protein transport inhibitor for 8 hours and IFN-γ was detected by

intracellular staining for flow cytometry. Data are representative for at least 2 independent experiments. Errors bars indicate ±SEM.